S. Širca, U Ljubljana (sirca@jlab.org) Ljubljana, March 14, 2013

WACS writeup 1: setting up the MC simulation

I have written a simple Monte-Carlo for the planned Wide-Angle (real) Compton Scattering (WACS) experiment in Hall C with a calorimeter (CALO) at beam-right and a High-Momentum Spectrometer (HMS) at beam-left. The first purpose of this document is to establish the RCS count rates of Bogdan's tentative 8- and 10-GeV kinematics [1] and to study the backgrounds, multiple scattering effects, and energy losses in a more detailed manner, as well as to optimize the CALO drift distance.

Two major settings are planned called "A" and "B":

$$E_\gamma = 8\,\mathrm{GeV}\,, \quad (s = 15.9\,\mathrm{GeV}^2)\,,$$

and

$$E_\gamma = 10\,\mathrm{GeV}\,, \quad (s = 19.6\,\mathrm{GeV}^2)\,,$$

the details of which are given in Tables 1 and 2. A general cartoon of the setup is shown in Fig. 1. Any particular kinematics in the text is referred to by the angle of the final photon, e.g. "A28" means setting "A" and $\theta_\gamma = 28^\circ$.

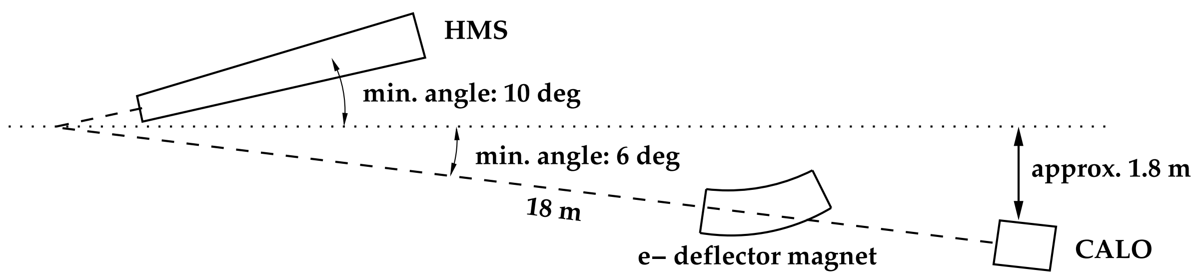

Figure 1: General layout of the WACS setup indicating the extreme forward angles of CALO and HMS that will be needed. The electrons from the elastic scattering on LH2 will be partly deflected by a sweeper magnet with a line strength of $\int \vec{B}\cdot \mathrm{d}\vec{l} \approx 0.3\,\mathrm{Tm}$.

The **fixed simulation parameters** are:

- $I_{\mathrm{beam}} = 40\,\mu\mathrm{A}$, 15 cm LH2 target (luminosity $\mathcal{L}_{\mathrm{ep}} = 1.58 \cdot 10^{38}/\mathrm{cm}^2\mathrm{s}$)
- $t_{\mathrm{rad}}/X_0 = 0.06$ Cu radiator, but actually use 0.08 due to additional radiative processes in the target and virtual photon flux
- front face CALO width = CALO height = 0.697 m
- rectangular-shape approximation of HMS colli, with horizontal opening = 6.4 cm (total width), vertical = 16.4 cm (total height), distance to HMS colli = 1.26 m, yielding a fixed $\Delta\Omega_{\mathrm{p}} = 6.5\,\mathrm{msr}$ (approx. $\pm 1.5^\circ$ horizontal, $\pm 3.7^\circ$ vertical)
- HMS momentum bite = $\pm 9\,\%$ around central momentum

0.1 Details of setting A

Table 1: Rate estimates for the $E_\gamma = 8\,\text{GeV}$ ($s = 15.9\,\text{GeV}^2$) RCS setting. The two lines for the RCS count rate $\dot{N}_{\text{RCS}}$ correspond to different ranges for the randomization of the incoming photon energy according to Eqs. (2) and (5), respectively. The rate of elastic electrons $\dot{N}_{\text{e}}$ implies a $\int \vec{B} \cdot \text{d}\vec{l} \approx 0.3\,\text{Tm}$ sweeper magnet.

$E_\gamma = 8\,\text{GeV}$ ($s = 15.9\,\text{GeV}^2$)										
$\theta_{\gamma'}$ [°]	7	11	15	19	28	33	40	48	55	
E'_γ [GeV]	7.522	6.917	6.199	5.463	4.004	3.368	2.671	2.094	1.726	
θ_{p} [°]	59.77	47.47	38.57	32.10	22.83	19.51	16.09	13.27	11.40	
p_{p} [GeV/c]	1.061	1.791	2.574	3.347	4.844	5.491	6.196	6.780	7.151	
d_{C} [m]	15	9.5	6.6	4.4	2.3	1.9	1.3	1	0.7	
J^{-1}	25.2	10.1	4.5	2.3	0.63	0.36	0.18	0.094	0.058	
$-t$ [GeV^2]	0.90	2.03	3.38	4.76	7.50	8.69	10.00	11.08	11.77	
$\dot{N}_{\text{RCS}}$ [h^{-1}]	54000	4200	960	380	123	84	61	48	41	Eq. (2)
$\dot{N}_{\text{RCS}}$ [h^{-1}]	226000	17700	4000	1570	412	250	159	113	92	Eq. (5)
$\dot{N}_{\text{e}}$ [h^{-1}]					926	766	737	525	837	

0.2 Details of setting B

Table 2: Rate estimates for the $E_\gamma = 10\,\text{GeV}$ ($s = 19.6\,\text{GeV}^2$) RCS setting. Notation as in Table 1.

$E_\gamma = 10\,\text{GeV}$ ($s = 19.6\,\text{GeV}^2$)										
$\theta_{\gamma'}$ [°]	6	10	14	18	24	30	36	40	45	52
E'_γ [GeV]	9.448	8.607	7.596	6.572	5.205	4.119	3.295	2.863	2.426	1.962
θ_{p} [°]	58.58	44.44	34.94	28.44	21.98	17.75	14.79	13.26	11.70	9.98
p_{p} [GeV/c]	1.157	2.135	3.208	4.264	5.656	6.754	7.586	8.021	8.460	8.927
d_{C} [m]	18	10	6.5	4.3	2.7	1.9	1.3			
J^{-1}										
$-t$ [GeV^2]	1.04	2.62	4.51	6.43	9.00	11.04	12.58			
$\dot{N}_{\text{RCS}}$ [h^{-1}]										
$\dot{N}_{\text{RCS}}$ [h^{-1}]	49000	3060	664	257	98	48	31			
$\dot{N}_{\text{e}}$ [h^{-1}]										

0.3 One particular kinematics

Let us focus on the following central kinematics (A28):

$$E_\gamma^{\rm c} = 8\,{\rm GeV}\,, \quad \theta_\gamma = 28^\circ\,, \quad E'_\gamma = 4.004\,{\rm GeV}\,, \quad \theta_{\rm p} = 22.83^\circ\,, \quad p_{\rm p} = 4.844\,{\rm GeV/c}\,, \tag{1}$$

with CALO placed at drift

$$d_{\rm C} = 2.3\,{\rm m}\,.$$

The incoming photon energy has been chosen according to the $1/E_\gamma$ spectrum in the range

$$E_\gamma^{\rm min} = 0.95\,E_\gamma^{\rm c}\,, \quad E_\gamma^{\rm max} = 1.05\,E_\gamma^{\rm c}\,, \tag{2}$$

so the energy of the incoming photon was randomized as

$$E_\gamma = \exp\left[\frac{\mathcal{R}}{\mathcal{N}} + \log E_\gamma^{\rm min}\right]\,, \quad \mathcal{N} = \left[\log\left(E_\gamma^{\rm max}/E_\gamma^{\rm min}\right)\right]^{-1}\,. \tag{3}$$

where $\mathcal{R}$ is uniformly distributed on $[0,1]$. The resulting event distributions are shown in Fig. 2.

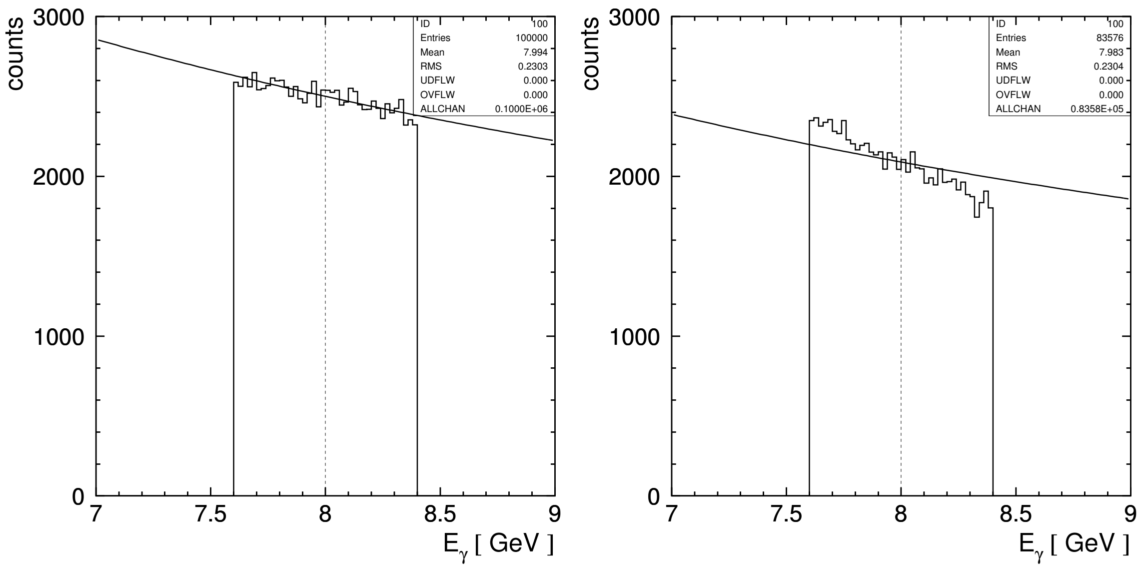

Figure 2: Event distribution in E_γ. [LEFT] Distribution of photons according to (3) within the ranges (2). The $1/E_\gamma$ function is also shown (scaled simply by eye). [RIGHT] Distribution of *accepted* photons (coincident with protons) in kinematics (1). It no longer has the characteristic $1/E_\gamma$ shape.

The distributions in the variables

$$s = M(M + 2E_\gamma)$$

and

$$t = 2E_\gamma E'_\gamma(\cos\theta - 1)$$

for kinematics (1), which corresponds to $s = 15.9\,{\rm GeV}^2$ and $t = -7.5\,{\rm GeV}^2$, are shown in Fig. 3.

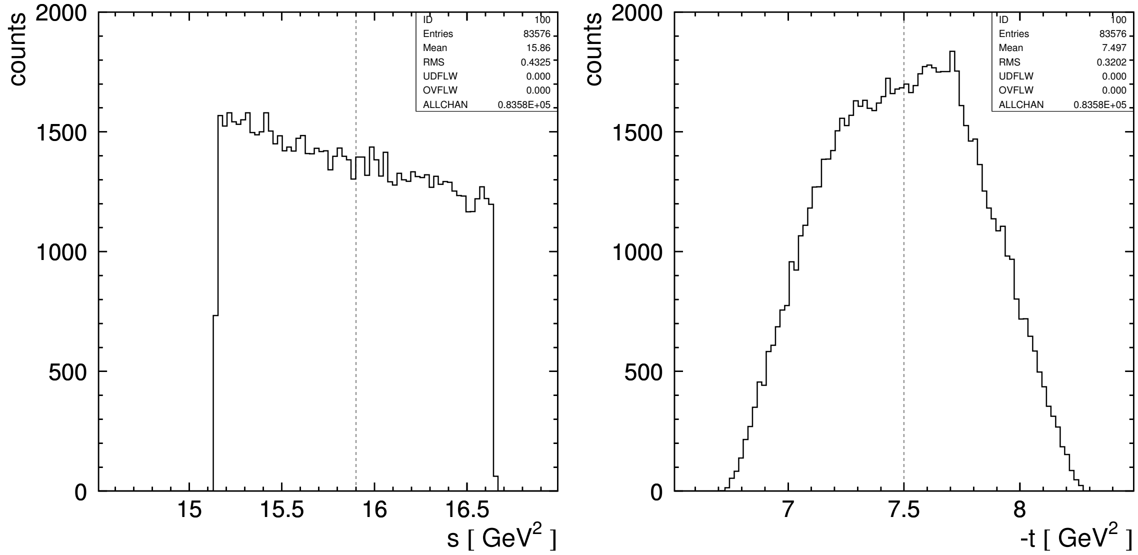

Figure 3: Distribution of accepted events in kinematics (1). [LEFT] Distribution in s. [RIGHT] Distribution in t.

The event distribution in the CALO and the HMS for kinematics (1) and $d_C = 2.3\,\mathrm{m}$ is shown in Fig. 4 (left). It is clear that purely from the standpoint of number of coincidences this is not the optimal setup: the CALO appears to be placed too close to the target as the number of photon singles is much larger than the number of coincidences (i.e. HMS determines the coincidence acceptance). Figure 5 shows the number of coincidences (unnormalized) as a function of drift distance. The number of coincidences starts to drop exactly at the point where the CALO and HMS acceptances match. The event distribution for $d_C = 3.9\,\mathrm{m}$ (just slightly below the optimum) is shown in Fig. 4 (right). The CALO drift distance will be optimized later.

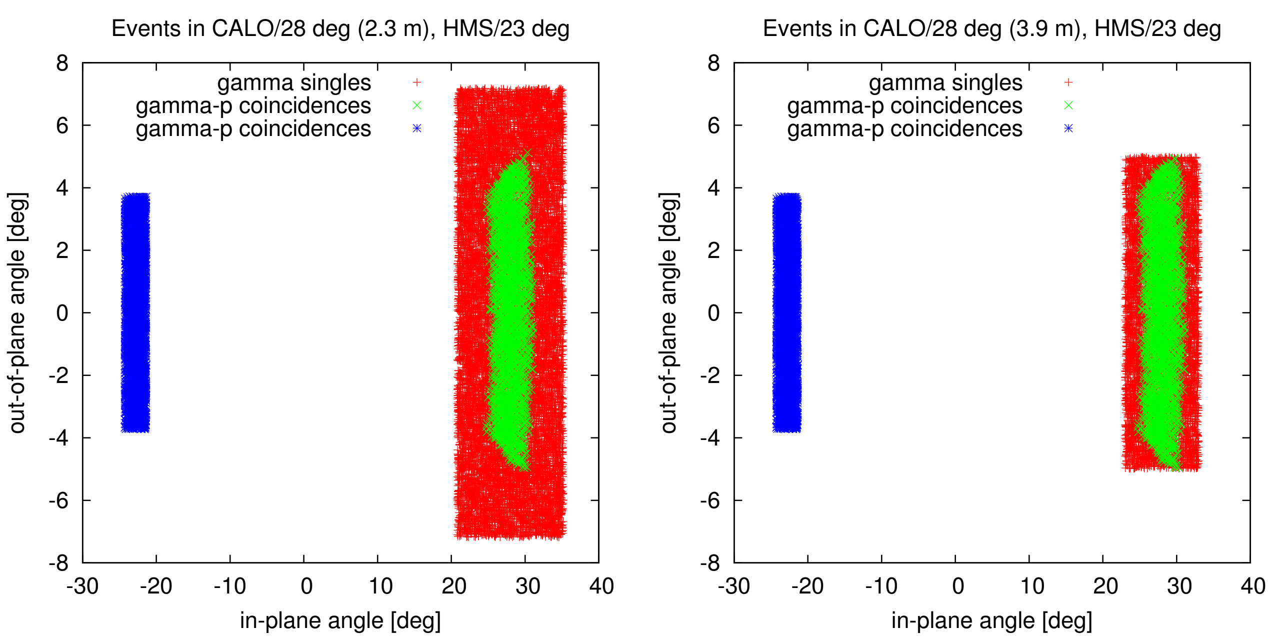

Figure 4: Event distribution for kinematics (1). [LEFT] 2.3 m CALO drift. [RIGHT] 3.9 m CALO drift. Note that this picture will change if E_γ is randomized in a range that is broader than (2).

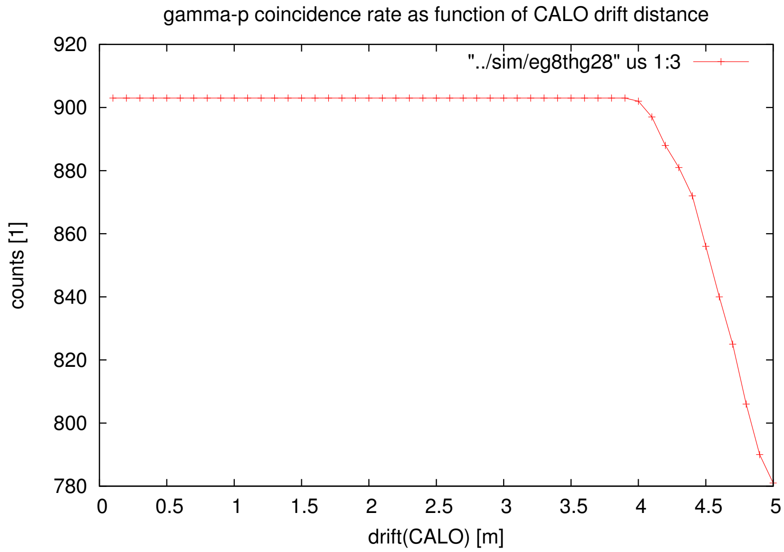

Figure 5: Unnormalized γ-p coincidence rate as function of CALO drift distance for kinematics (1).

0.4 The RCS counting rate

The Compton counting rate is given by

$$\dot{N}_{\rm RCS} = \frac{\mathrm{d}\sigma_{\rm RCS}(s)}{\mathrm{d}t}\Big[\frac{E_\gamma'^2}{\pi}\underbrace{\Delta\Omega_{\rm p}\frac{\mathrm{d}\Omega_\gamma}{\mathrm{d}\Omega_{\rm p}}}_{\Delta\Omega_\gamma}\Big] f_{\gamma\rm p}\left[\frac{\Delta E_\gamma}{E_\gamma}\frac{t_{\rm rad}}{X_0}\right]\mathcal{L}_{\rm ep}\,. \tag{4}$$

According to Brodsky the RCS cross-section should scale as $1/s^2t^4$ at high s and high t, so I have used the existing RCS data at $s = 10.92\,\mathrm{GeV}^2$ taken during the E99-114 experiment [2] (see Fig. 6) by a $1/t^4$ function.

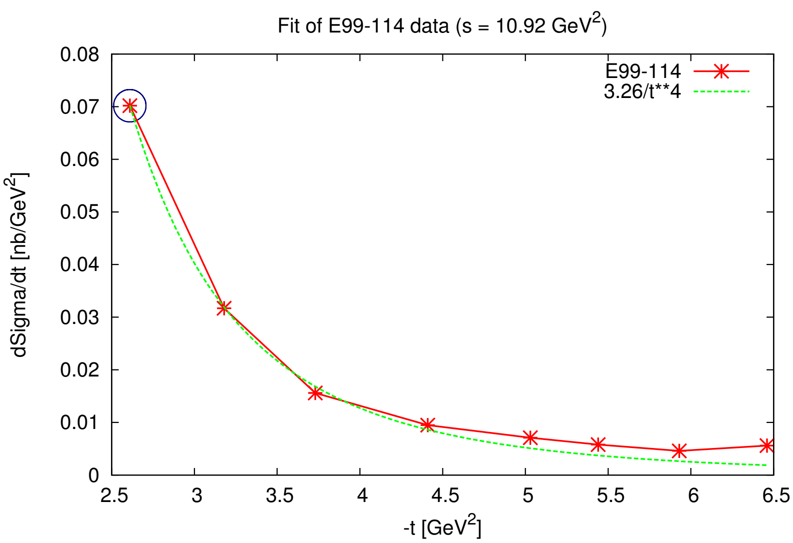

Figure 6: Fit of the highest-s ($10.92\,\mathrm{GeV}^2$) differential cross-sections measured in E99-114 with a $1/t^4$ dependence. The last data point was omitted from the fit.

Although the data do not seem to support this fit optimally, I have used the following simple formula to predict the WACS cross-section at higher s:

$$\frac{d\sigma}{dt}(s,t) = 3.26 \left(\frac{s_0}{s}\right)^2 \frac{1}{t^4} \left[\frac{\text{nb}}{\text{GeV}^2}\right] , \quad s_0 = 10.92\,\text{GeV}^2 ,$$

where s and t are in GeV^2. Alternatively, one can pick a single point on the graph (e.g. the one at $-t = 2.61\,\text{GeV}^2$, blue circle in Fig. 6) and use it as the reference. In this case, the fit formula becomes

$$\frac{d\sigma}{dt}(s,t) = 0.0702 \left(\frac{s_0}{s}\right)^2 \left(\frac{t_0}{t}\right)^4 \left[\frac{\text{nb}}{\text{GeV}^2}\right] , \quad s_0 = 10.92\,\text{GeV}^2 , \quad -t_0 = 2.61\,\text{GeV}^2 .$$

Because the first fit passes almost exactly through the point at $-t = 2.61\,\text{GeV}^2$, the difference between these empirical expressions is negligible.

In kinematics (1) we have $s = 15.9\,\text{GeV}^2$, hence the central value of the cross-section is

$$\frac{d\sigma}{dt}(s = 15.9, t = -7.5) \approx 0.486\,\text{pb}/\text{GeV}^2 ,$$

while in the simulation it is calculated on the fly. The cross-section variation across the acceptance is quite large (see Fig. 7).

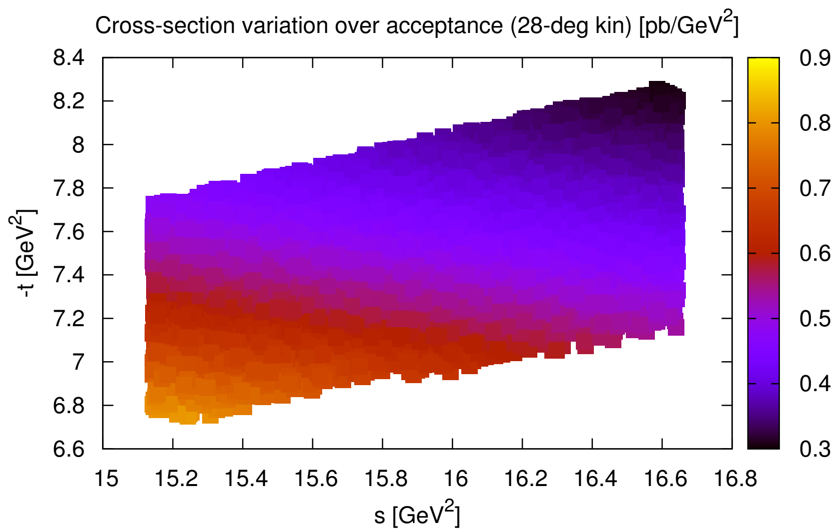

Figure 7: Cross-section variation over the acceptance for kinematics (1).

The Jacobian in (4) which, of course, is effectively (not explicitly) included in the simulated, is given by

$$J = \frac{d\Omega_\gamma}{d\Omega_p} = \frac{d(\cos\theta_\gamma)}{d(\cos\theta_p)} = -\frac{4A\cos\theta_p}{(A + \cos^2\theta_p(1-A))^2} , \quad A = \left(1 + \frac{E_\gamma}{m_p}\right)^2 .$$

Note that in [1] this is denoted as $J_h \times J_v = J^{-1}$. Moreover, in my MC we have $f_{\gamma p} = 1$ as I am looking only at coincidence events. With all the above numbers and assumptions I obtain

$$\dot{N}_{\text{RCS}} = 123\,/\text{hour}$$

in kinematics (1). The rates for other settings are listed in Tables 1 and 2.

0.5 Finding the correct range of E_γ

Randomizing the incoming photon according to the range (2) has been chosen arbitrarily. To see how the allowed range in p_p (given by the HMS momentum bite) translates to the range in E_γ, I have used the relations

$$E'_\gamma = \frac{E_\gamma}{1 + \frac{E_\gamma}{m_\mathrm{p}}(1-\cos\theta)} \,, \qquad E_\mathrm{p} = E_\gamma - E'_\gamma + m_\mathrm{p} \,, \qquad p_\mathrm{p} = \sqrt{E_\mathrm{p}^2 - m_\mathrm{p}^2} \,,$$

and computed the Jacobian

$$\frac{\mathrm{d}p_\mathrm{p}(E_\gamma)}{\mathrm{d}E_\gamma} = \cdots \,,$$

but it is ugly and depends on θ, i.e. the range in E_γ needed to cover the accepted range in p_p can NOT be computed simply by

$$\Delta E_\gamma \approx \left(\frac{\mathrm{d}p_\mathrm{p}(E_\gamma)}{\mathrm{d}E_\gamma}\right)^{-1} \Delta p_\mathrm{p} \,.$$

To see what the required ranges are, I have randomized the incoming photon according to a much broader range

$$E_\gamma^\mathrm{min} = 0.10\,E_\mathrm{e} \,, \quad E_\gamma^\mathrm{max} = 1.00\,E_\mathrm{e} \,, \quad E_\mathrm{e} = 10\,\mathrm{GeV} \,,$$

i.e. all the way to the formal endpoint (beam) energy, assumed to be 10 GeV, and observed the corresponding span in p_p. The resulting distribution of γ-p coincidence events is shown in Fig. 8 for all nine "A" kinematics.

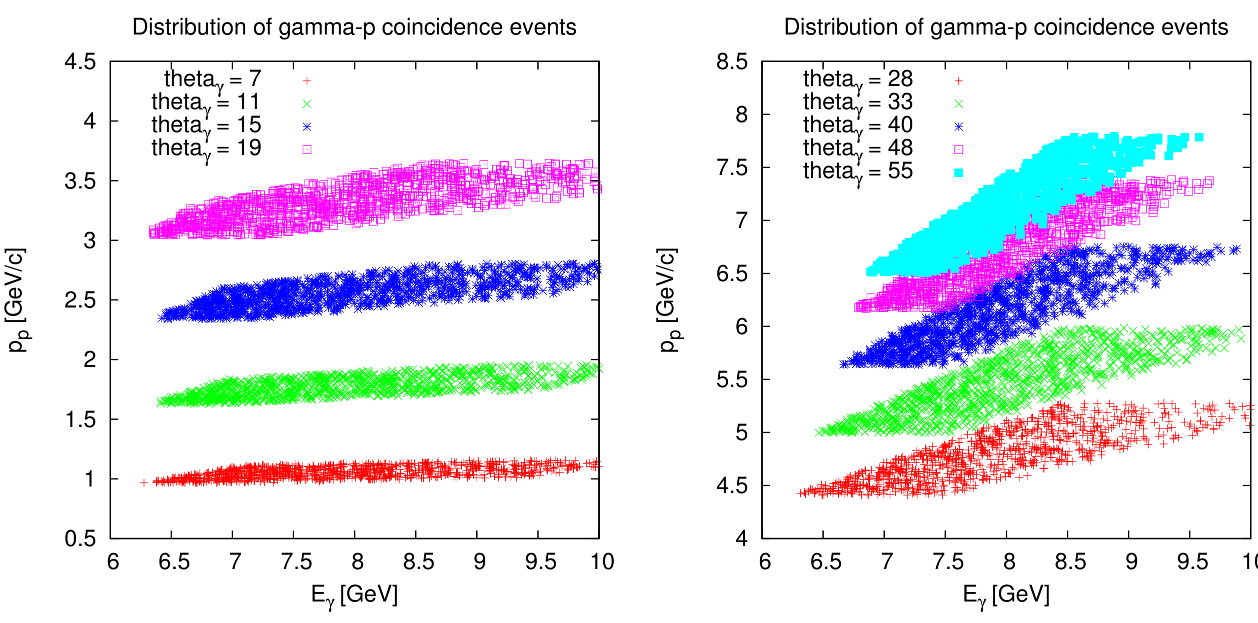

Figure 8: Distribution of E_γ vs. p_p for accepted coincidence events in kinematics "A" (see Table 1). [LEFT] Angles 7° to 19°. [RIGHT] Angles 28° to 55°.

Note that in each setting, the events tend to accumulate strongly at the low-p_p, low-E_γ portion of each trapezoid, so it is particularly important to include the lower portion of the $1/E_\gamma$ spectrum. For the subsequent rate estimates I have assumed

$$E_\gamma^\mathrm{min} = 0.62\,E_\mathrm{e} \,, \quad E_\gamma^\mathrm{max} = 1.00\,E_\mathrm{e} \,, \quad E_\mathrm{e} = 10\,\mathrm{GeV} \qquad (5)$$

instead of (2). This results in quite different rates which are listed in Table 1.

0.6 Simulation of elastic electron scattering

I have assumed an incoming beam of $E_{\mathrm{e}} = 10\,\mathrm{GeV}$. Then the HMS at 22.83° (still sticking to kinematics (1)) will see the recoiled protons, while the CALO positioned at 28° will see the elastically scattered electrons in addition to the desired RCS photons, unless they are cleared away or at least deflected by a sweeper magnet. The deflection angle of the sweeper magnet is given approximately by

$$\text{deflection} = \frac{0.3 \int \vec{B} \cdot \mathrm{d}\vec{l}}{p\,[\mathrm{GeV}/c]} .$$

Presently a sweeper magnet is available with

$$\int \vec{B} \cdot \mathrm{d}\vec{l} \approx 0.3\,\mathrm{Tm} ,$$

and this is the value I have used in the simulations. I have assumed the standard dipole parameterizations of $G_{\mathrm{E}}^{\mathrm{p}}$ and $G_{\mathrm{M}}^{\mathrm{p}}$ when computing the elastic cross-section.

0.7 Incorporating the resolutions

Energy loss of protons

In kinematics (1), we have $p_{\mathrm{p}} \approx 4.8\,\mathrm{GeV}/c$. In other settings of the $E_\gamma = 8\,\mathrm{GeV}$ ($s = 15.9\,\mathrm{GeV}^2$) setup, the proton momenta range from ≈ 1 to $\approx 7\,\mathrm{GeV}/c$, for which the specific energy loss in LH2 is

$$\frac{\mathrm{d}E_{\mathrm{p}}}{\mathrm{d}x} \approx -5\,\mathrm{MeV/g\,cm^{-2}} .$$

For the 2-inch cylindric LH2 target, the mean path of protons is 1 inch, thus

$$\Delta E_{\mathrm{p}} \approx -0.9\,\mathrm{MeV} \qquad (\text{protons in 1 inch LH2}) .$$

Similarly,

$$\Delta E_{\mathrm{p}} \approx -0.3\,\mathrm{MeV} \qquad (\text{protons in 1.26m air}) ,$$

hence

$$\Delta E_{\mathrm{p}} \approx -1.2\,\mathrm{MeV} \qquad (\text{total}) ,$$

The straggling of these losses is supposed to be Gaussian with a sigma of 1/4 of the above total number ($\approx 0.3\,\mathrm{MeV}$).

Multiple scattering of protons

The spread of the scattering angle for protons with momentum p_{p} traversing a material with thickness x is

$$\theta_0 \approx \frac{13.6\,\mathrm{MeV}}{\beta_{\mathrm{p}} c p_{\mathrm{p}}} \sqrt{\frac{x}{X_0}} , \tag{6}$$

where X_0 is the radiation length: $X_0(\mathrm{LH2}) = 866\,\mathrm{cm}$ and $X_0(\mathrm{air}) = 30420\,\mathrm{cm}$. This does not amount to much. The total effect at the location of the HMS collimator is shown in Fig. 9 (left).

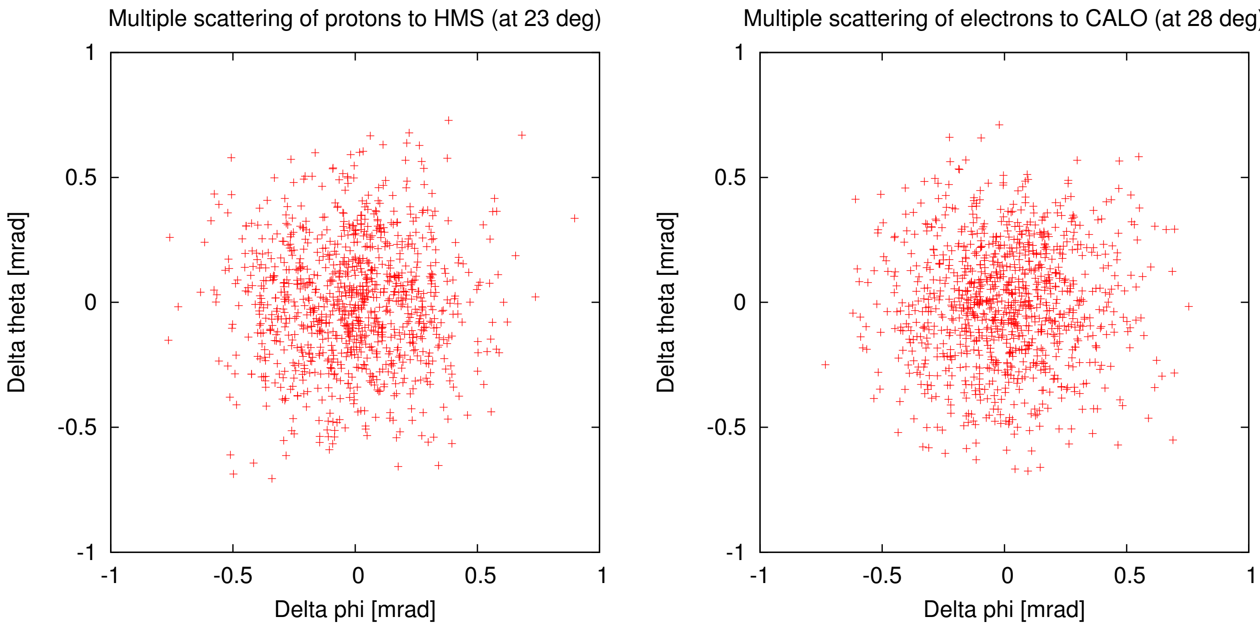

Figure 9: [LEFT] Effect of multiple scattering of protons in LH2 and air, just prior to entering the HMS collimator, for kinematics 1. [RIGHT] Same for elastic electrons (assuming 10 GeV beam energy) just prior to entering the CALO.

Energy loss of elastic electrons

By using the same energy loss formulas as above, typical losses are

$$\Delta E_{\mathrm{e}} \approx -0.7\,\mathrm{MeV} \qquad \text{(electrons in 1 inch LH2)}$$

and

$$\Delta E_{\mathrm{e}} \approx -2.6 \cdot 10^{-4}\,\mathrm{GeV/m} \qquad \text{(electrons in air)}\,.$$

Multiple scattering of elastic electrons

Use same formula as above, Eq. (6), with p_{p} and β_{p} replaced by p_{e} and β_{e}. The contribution of air changes with CALO drift distance. The total effect at the CALO front face is shown in Fig. 9 (right).

Resolution of photon and elastic electron detection in segmented CALO

The CALO is segmented in 34×34 blocks, each with a front-face surface area of $2.05\times 2.05\,\mathrm{cm}^2$. A naive assumption would be that the detection resolution for either the RCS photon or the elastically scattered electron is given simply by the block size, i.e.

$$\sigma_x \approx \sigma_y \approx 2\,\mathrm{cm}$$

in terms of linear dimensions, but this is too pessimistic. It has been shown in [3] that the position resolution for $1 \le E \le 5.5\,\mathrm{GeV}$ can be parameterized as

$$\sigma_x(E)\,[\mathrm{cm}] \approx 0.039 + \frac{0.522}{\sqrt{E\,[\mathrm{GeV}]}}\,,$$

so that it is typically between 0.5 and 0.3 cm in the energy range given above. In the following I will assume that this parameterization applies also to higher energies. The resulting event distributions for two settings ($\theta_\gamma = 28^\circ$ and $\theta_\gamma = 48^\circ$) are shown in Fig. 10.

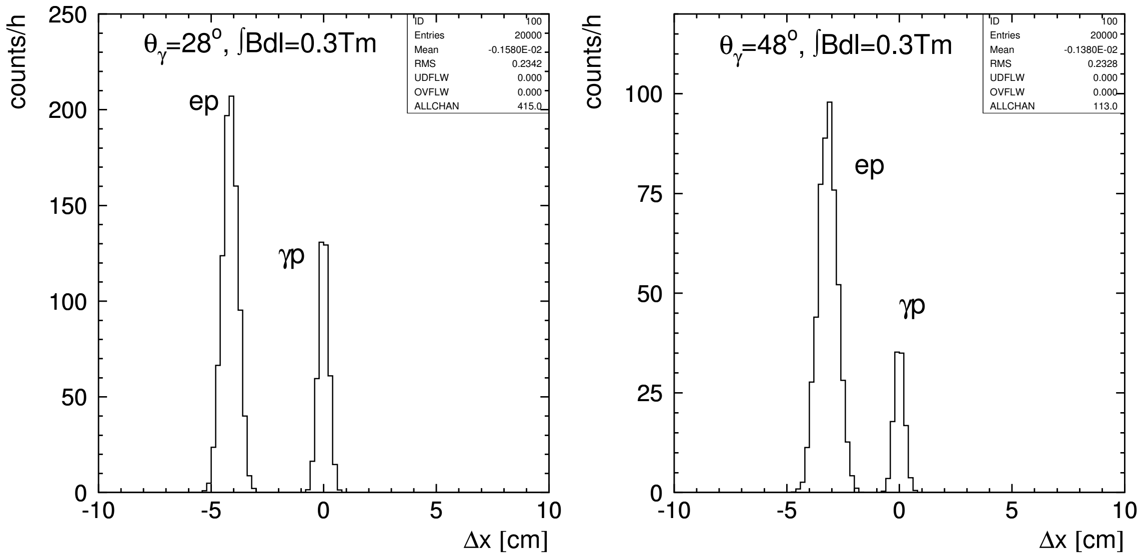

Figure 10: Distribution of accepted events in CALO for [LEFT] CALO at nominal angle $\theta_\gamma = 28^\circ$ (kinematics (1)) and [LEFT] CALO at nominal angle $\theta_\gamma = 48^\circ$.

0.8 CALO drift distance optimization

Figure 11 shows the ratio of γ-p coincidences and γ singles in CALO as a function of CALO drift distance, for the proposed $E_\gamma = 8$ GeV kinematics.

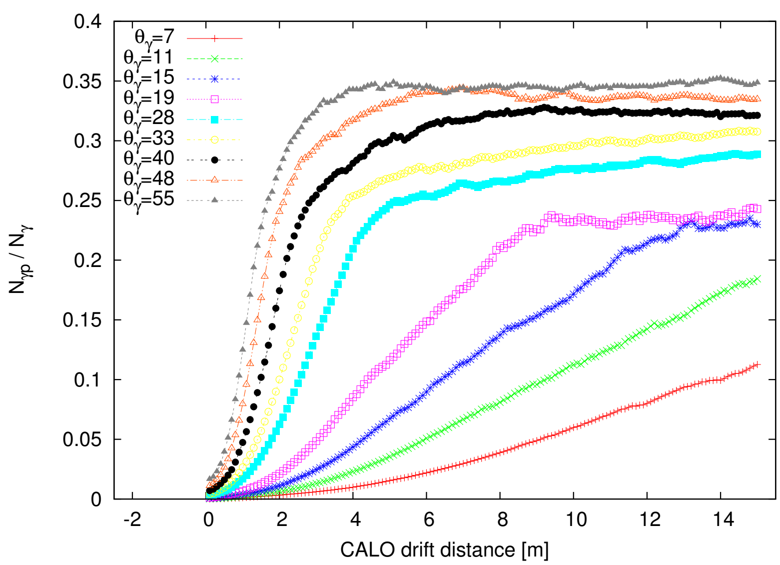

Figure 11: The ratio of γ-p coincidences and γ singles in CALO as a function of CALO drift distance, for the kinematics listed in Table on page 20 of [1].

But $N_{\gamma p}/N_\gamma$ is not the only relevant quantity. The optimal drift distance depends on several criteria. By placing the CALO too close to the target, the HMS determines the coincidence acceptance and there are too many γ singles; angular resolution deteriorates; the spatial difference between the electrons from e-p elastic scattering and photons from RCS becomes very small (with the additional constraint that the sweeper magnet needs to be placed between the target and the CALO, occupying about 1 m). The optimization procedure consists of trying to find a drift distance such that as many coincidences as the CALO geometry allows are accepted without letting the peaks in Fig. 10 to merge. This is work in progress.

References

[1] B. Wojtsekhowski, *Wide-angle Compton scattering up to* 10 GeV, Hall C Users Meeting, JLab, January 24, 2013.

[2] A. Danagoulian et al. (Hall A Collaboration), Phys. Rev. Lett. **98** (2007) 152001.

[3] M. A. P. Carmignotto, *Neutral Particle Detector: Simulations*, Hall C Users Meeting, JLab, January 24, 2013.